Acta Crystallographica Section A
Foundations of Crystallography
ISSN 0108-7673

Received 21 April 2008
Accepted 25 June 2008

Measurement of X-ray rocking curves in the Bragg–Laue case

Masami Yoshizawa,[a]* Tomoe Fukamachi,[a] Kenji Hirano,[a] Tsuyoshi Oba,[a] Riichirou Negishi,[a] Keiichi Hirano[b] and Takaaki Kawamura[c]

[a]Saitama Institute of Technology, 1690 Fusaiji, Fukaya, Saitama 369-0293, Japan, [b]Institute of Material Structure Science, KEK-PF, High Energy Accelerator Research Organization, Oho-machi, Tukuba, Ibaraki 305-0801, Japan, and [c]Department of Mathematics and Physics, University of Yamanashi, Kofu, Yamanashi 400-8510, Japan. Correspondence e-mail: yoshizaw@sit.ac.jp

X-ray rocking curves in the Bragg–Laue case diffracting from the side surface of a plane-parallel crystal have been measured using a high-resolution optical system. The full width at half-maximum of the rocking curves is approximately three times narrower than that measured from the top surface. The characteristics of the transmitted beam from the side surface are almost the same as those through a thin crystal in the Bragg case. The rocking curves and the direction of X-ray energy flow in the crystal observed in the experiment can be reproduced using Wagner's approach [Wagner (1956), *Z. Phys.* **146**, 127–168].

1. Introduction

X-rays diffracted from the side surface of a thin plane-parallel crystal have been observed when the effective linear absorption coefficient μ becomes a minimum owing to the Borrmann effect (Fukamachi *et al.*, 2004, 2005). Enhancement of these diffracted beam intensities has been observed by increasing the width of the incident X-rays (Fukamachi *et al.*, 2004). Fukamachi *et al.* (2006) have explained that this enhancement is caused by the confined beam which propagates in a thin crystal in addition to the diffracted beam from the top surface and the transmitted beams through the bottom surface. The diffraction scheme propagating in a thin crystal may be called the Bragg–(Bragg)^m case (BB^m case, for short); the first Bragg represents the initial diffraction in the Bragg case and the second (Bragg)^m represents a sequence of 'm' times diffractions in the Bragg case at the top and bottom surfaces. If the crystal size is finite, the confined beam may exit from a side surface. This diffraction scheme is called the Bragg–(Bragg)^m–Laue case (BB^{m}L case, for short) as the last diffraction from the side surface is in the Laue case. In the BB^{m}L case, interference fringes have been observed in the diffracted beam from the side surface (Fukamachi *et al.*, 2004, 2005). When m = 0 in the BB^{m}L case, the diffraction scheme is represented by the Bragg–Laue case (BL case, for short).

Borrmann *et al.* (1955) first carried out an experiment in the BL case. They measured diffraction from the side surface of a crystal when μ became a minimum owing to anomalous transmission (Borrmann effect). Authier (1962, 2001) also carried out an experiment in the BL case and pointed out theoretically by using Wagner's approach (Wagner, 1956) that the diffracted curve from the crystal surface corresponded to that from an infinitely thick crystal as the bottom surface did not influence the diffraction.

In this paper we report measurements of rocking curves in the BL case using X-rays from synchrotron radiation with a very high resolution optical system. We compare the measured curves with those calculated using Wagner's approach which is based on Laue's dynamical theory of diffraction.

2. Experiment

The experiment was carried out at beamline 15C, Photon Factory (PF), KEK, Japan. A schematic diagram of the measuring system is shown in Fig. 1. X-rays from synchrotron radiation were monochromated by an Si 111 double-crystal monochromator, a Ge 220 monochromator and a Ge 220 asymmetric monochromator [the asymmetry factor (Negishi *et al.*, 2008) was 22]. The X-rays were σ-polarized and their energy was 11100 $\pm$ 0.5 eV, which was 3 eV below the Ge K-absorption edge (11103 eV). The vertical and horizontal widths of the incident beam after slit 2 were adjusted to be 20 μm and 500 μm, respectively. The thickness of the sample

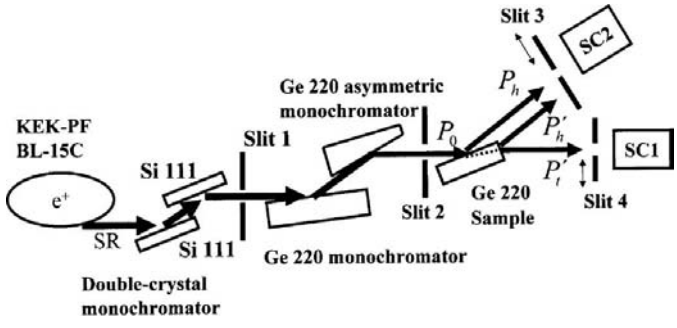

Figure 1
Schematic diagram of the measuring system. SR = synchrotron radiation, SC = scintillation counter.

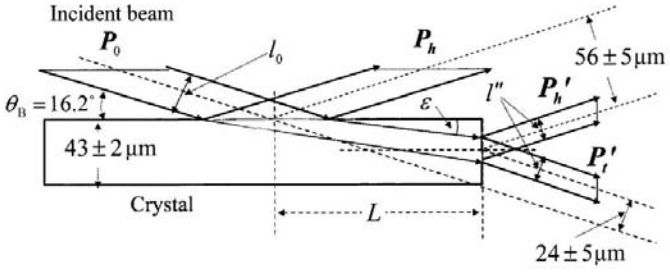

Figure 2
Schematic diagram of the beam arrangement in the present experiment.

crystal was 43 μm. Rocking curves of the Ge 220 reflection in the BL case were measured. Fig. 1 shows the directions of the incident beam P_0, the diffracted beam P_h, and the diffracted and transmitted beams from the side surface P_h' and P_t', respectively. An outline of the diffraction geometry in the measurement is shown in Fig. 2. The distance between the peaks of P_h and P_h' was measured by moving slit 3 and was determined to be 56 ± 5 μm as shown in Fig. 3. Fig. 4 shows the measured rocking curves of P_h, P_h' and P_t'. These intensities are normalized so as to show the same peak height. The abscissa is the angle deviation from the exact Bragg condition. The center of the rocking curve is taken at the exact Bragg angle for P_h. The peak positions of P_h' and P_t' are located 4 arcsec to the lower side of the peak of P_h. The full width at

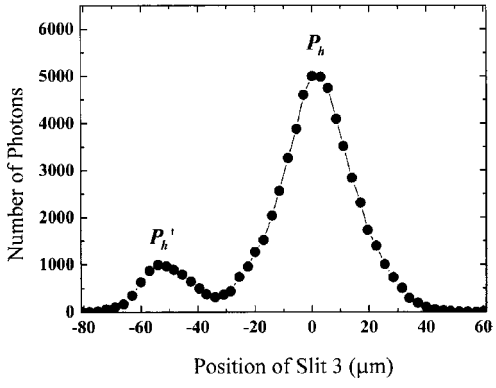

Figure 3
Measurement of distance between P_h and P_h'.

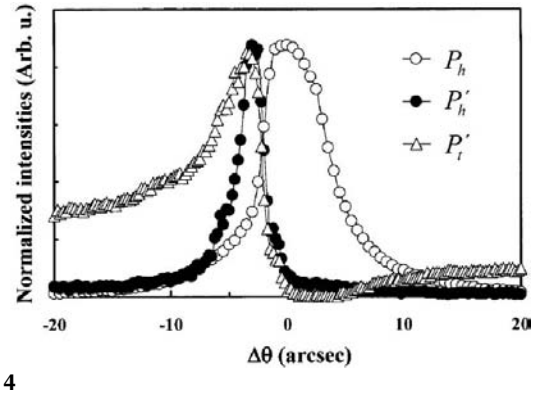

Figure 4
Measured rocking curves of P_h, P_h' and P_t' in the Bragg–Laue case as a function of the angle deviation $\Delta\theta$ from the Bragg condition.

half-maximum (FWHM) of P_h is 6.5 arcsec, and the curve of P_t' has a higher background on the low-angle side of the peak. The FWHM of P_h' is 2.5 arcsec and is the narrowest among these three curves.

Incident-beam X-rays without a sample (P_0) were measured by scintillation counter SC1, then the transmitted X-rays scattered out from the side surface (P_t') were measured by moving slit 4 when the Ge 220 Bragg condition was satisfied. The distance between the beam positions P_0 and P_t' was 24 ± 5 μm, as shown in Fig. 2. The refractive angle ε_m (Fig. 2) of the effective refracted beam in the crystal when the intensity of P_h' was a maximum was 6.6 ± 2°. Then the distance of the incident point of the X-rays from the side edge of the sample was estimated to be $L = 143 \pm 18$ μm, which agreed with the actual length in the measurement.

3. Calculation of rocking curves

We define χ_h as the Fourier transform of the X-ray polarizability $\chi(\mathbf{r})$ as given by

$$\chi_h = \chi_{hr} + i\chi_{hi} = |\chi_{hr}| \exp(i\alpha_{hr}) + i|\chi_{hi}| \exp(i\alpha_{hi}). \quad (1)$$

Here χ_{hr} and χ_{hi} are Fourier transforms of the real and imaginary parts of $\chi(\mathbf{r})$, respectively. According to the book by Authier (2001), the intensity ratios P_h/P_0, P_h'/P_0 and P_t'/P_0 are given by

$$P_h/P_0 = \left|r^{(1)}\right|^2, \quad (2)$$

$$P_h'/P_0 = (l''/l_0)|r^{(1)}|^2 \exp(-\mu z/\sin\varepsilon), \quad (3)$$

$$P_t'/P_0 = (l''/l_0) \exp(-\mu z/\sin\varepsilon), \quad (4)$$

where μ is the effective linear absorption coefficient under dynamical diffraction, and the angle $\varepsilon = \tan^{-1}(z/L)$ is shown in Fig. 2. The beam-size correction l''/l_0 is given by

$$\frac{l''}{l_0,} = \tan\varepsilon \cot\theta_B = \frac{1 - \left|r^{(1)}\right|^2}{1 + \left|r^{(1)}\right|^2}, \quad (5)$$

where θ_B is the Bragg angle, and l_0 and l'' are the sizes of the incident and diffracted beams from the side surface, respectively, as shown in Fig. 2. In equation (5),

$$r^{(1)} = \frac{\left(|\chi_{hr}|^2 + |\chi_{hi}|^2\right)^{1/2}}{\chi_{-h}}\left[-(W + ig) - B^{1/2}\right], \quad (6)$$

$$g = \chi_{0i}/\left(|\chi_{hr}|^2 + |\chi_{hi}|^2\right)^{1/2} = -k\left(1 + k^2\right)^{-1/2}, \quad (7)$$

$$B^{1/2} = \left[(W + ig)^2 - \exp(2i\theta)\right]^{1/2}, \quad (8)$$

$$k = |\chi_{hi}|/|\chi_{hr}|, \quad (9)$$

$$\theta = \tan^{-1}(k\cos\delta), \quad (10)$$

$$\delta = \alpha_{hi} - \alpha_{hr}. \quad (11)$$

W is the deviation parameter (Fukamachi *et al.*, 2002) given by

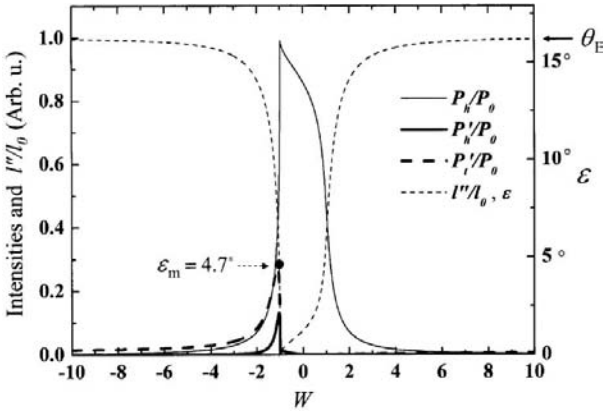

Figure 5
Calculated rocking curves of P_h/P_0, P_h'/P_0 and P_t'/P_0 in the Bragg–Laue case as a function of deviation parameter W from the Bragg condition. The values of the normal atomic scattering factor $f^0 = 23.77$, and the real and imaginary parts of the anomalous scattering factor, $f' = -9.08$ and $f'' = -1.13$, respectively (Yoshizawa *et al.*, 2005), were used, and $L = 143$ μm.

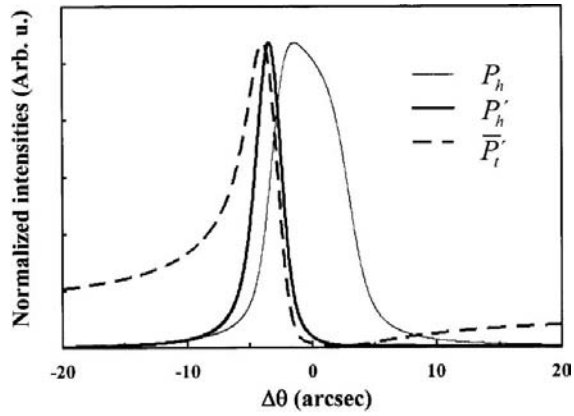

Figure 6
Calculated rocking curves of P_h, P_h' and $\bar{P}_t'$ in the Bragg–Laue case as a function of $\Delta\theta$ after thermal correction and convolution with the angular resolution in the experiment.

$$W \simeq \frac{\Delta\theta \sin^2\theta_B}{\left(|\chi_{hr}|^2 + |\chi_{hi}|^2\right)^{1/2}}, \tag{12}$$

where $\Delta\theta$ is the deviation angle from the Bragg angle in the crystal.

Fig. 5 shows the calculated curves of P_h/P_0, P_h'/P_0, P_t'/P_0, I''/I_0 and ε under the experimental conditions; the thermal correction is not included. The curve of P_h/P_0 in the BL case is the same as that in the Bragg case for a semi-infinite crystal. The curve of P_t'/P_0 has high background on both sides of the peak. The curve of P_h'/P_0 has a sharp peak. The curve of I''/I_0 becomes remarkably small in the region $-1.2 < W < 1$. The change in ε is the same as for the curve of I''/I_0 and varies from 0 to the Bragg angle θ_B. The value of ε_m at the peak position of P_h'/P_0 is 4.7°.

4. Discussion

In the present experiment the rocking curves of P_h, P_h' and P_t' in the BL case were measured. It is shown that the intensity of P_h' is approximately five times smaller than that of P_h, and the FWHM of the rocking curve of P_h' is three times smaller than that of P_h.

Since the shape of the curve of P_t' is very sensitive to the variation of the distance L in this experiment, it is better to include the correction for the incident-beam width. The averaged value $\bar{P}_t'$ is defined by

$$\bar{P}_t' = \left[P_t'(L + \Delta L) + P_t'(L) + P_t'(L - \Delta L)\right]/3,$$

where $\Delta L = 50$ μm in the present experiment. Fig. 6 shows the calculated rocking curves of P_h, P_h' and $\bar{P}_t'$ in the BL case, by taking thermal correction into account and by convoluting with the angular resolution of the optical system. In order to compare these with the measured results in Fig. 4, the intensities of the three rocking curves are normalized so as to show the same peak height. The calculated rocking curves in Fig. 6 show excellent agreement with the measured curves in Fig. 4.

The measured angle ε_m ($6.6 \pm 2°$) corresponds to the calculated value of $\varepsilon = \tan^{-1}(z/L)$ (4.7°) within experimental error. It is noted that ε_m corresponds to the angle between the incident surface and the Poynting vector in the crystal, which is known to be normal to the dispersion surface. It is acceptable that the effective refracted beam direction in the crystal is given by the Poynting vector, because the energy flow of the X-rays is given by the Poynting vector. These results clearly show that Wagner's approach is applicable to analysis of the diffraction in the BL case.

There are several possible applications of using diffraction in the BL case. One is, for example, to use P_h' as a high-resolution monochromator, because the FWHM of the rocking curve of P_h' is much smaller than that of P_h. In this monochromator the beam fluctuation of P_h' can be corrected by monitoring P_t', since the peak angles of P_h' and P_t' are very close to each other.

Another is to use the transmitted beam P_t' from the side surface as a phase-retarder, because the characteristics of P_t' are almost the same as those of the transmitted beam P_t in a thin plane-parallel crystal in the Bragg case, which has been used as a phase-retarder (Hirano *et al.*, 1992). In the conventional method, as the phase shift of the phase-retarder depends on the X-ray wavelength and the crystal thickness, which determines the X-ray path length, it is necessary to prepare thin plane-parallel crystals of different thicknesses according to the wavelength so as to obtain a suitable phase shift. In the present case, however, it is possible to obtain the optimum condition only by changing the distance L, which is much easier. This is certainly an advantage of using diffraction in the BL case.

The authors thank Professor M. Tokonami of Saitama Institute of Technology (SIT) for valuable discussions. They are grateful to Mr T. Tanaka for assistance in some of the experiments. This work was carried out under the approval of the Program Advisory Committee of PF (Proposal No. 2006G274). This work was partly supported by the 'High-Tech Research Center' Project for Private Universities: matching

fund subsidy from MEXT (Ministry of Education, Culture, Sports, Science and Technology), 1999–2003 and 2004–2007.

References

Authier, A. (1962). *J. Phys. Radium*, **23**, 961–969.
Authier, A. (2001). *Dynamical Theory of X-ray Diffraction*, pp. 341–344. Oxford University Press.
Borrmann, G., Hildebrandt, G. & Wagner, H. (1955). *Z. Phys.* **142**, 406.
Fukamachi, T., Negishi, R., Yoshizawa, M. & Kawamura, T. (2005). *Jpn. J. Appl. Phys.* **44**, L787–L789.
Fukamachi, T., Negishi, R., Yoshizawa, M. & Kawamura, T. (2006). *Jpn. J. Appl. Phys.* **45**, 2830–2832.
Fukamachi, T., Negishi, R., Yoshizawa, M. Sakamaki, T. & Kawamura, T. (2004). *Jpn. J. Appl. Phys.* **43**, L865–L867.
Fukamachi, T., Negishi, R., Zhou, S., Yoshizawa, M. & Kawamura, T. (2002). *Acta Cryst.* A**58**, 552–558.
Hirano, K., Ishikawa, T., Koreeda, S., Fuchigami, K., Kanazaki, K. & Kikuta, S. (1992). *Jpn. J. Appl. Phys.* **31**, L1209–L1211.
Negishi, R., Fukamachi, T., Yoshizawa, M., Hirano, K., Hirano, K. & Kawamura, T. (2008). *J. Phys. Soc. Jpn*, **77**, 023709.
Wagner, H. (1956). *Z. Phys.* **146**, 127–168.
Yoshizawa, M., Zhou, S., Negishi, R., Fukamachi, T. & Kawamura, T. (2005). *Acta Cryst.* A**61**, 553–556.